We are IntechOpen,
the world's leading publisher of
Open Access books
Built by scientists, for scientists

6,900
Open access books available

186,000
International authors and editors

200M
Downloads

Our authors are among the

154
Countries delivered to

TOP 1%
most cited scientists

12.2%
Contributors from top 500 universities

CLARIVATE ANALYTICS
BOOK CITATION INDEX
INDEXED

WEB OF SCIENCE™

Selection of our books indexed in the Book Citation Index
in Web of Science™ Core Collection (BKCI)

Interested in publishing with us?
Contact book.department@intechopen.com

Numbers displayed above are based on latest data collected.
For more information visit www.intechopen.com

Evaluation Method for Mean Stress Effect on Fatigue Limit of Non-Combustible Mg Alloy

Kazunori MORISHIGE, Yuna MAEDA,
Shigeru HAMADA and Hiroshi NOGUCHI
Department of Mechanical Engineering, Faculty of Engineering, Kyushu University
JAPAN

1. Introduction

Structures are commonly loaded with a mean stress. Therefore, it is necessary to investigate the influence of the mean stress on the fatigue strength of the structural materials. Fatigue strength of a material, whose fatigue crack is initiated from an inclusion, strongly depends on the size of the inclusion. The fatigue strength of the material is quite variable. Therefore, if we test the effect of the mean stress on the fatigue strength of this material, the effect would be hidden in the scatter and the effect becomes uncertain. In this study, we propose an evaluation method for the mean stress effect of the inclusion-induced scattered fatigue strength using the non-combustible Mg alloy AMX602B (X=Ca) (Sakamoto et al., 1997; Chang et al., 1998; Akiyama et al., 2000). We discuss the equivalence of an artificial defect and an actual defect (inclusion).

Figure 1 shows the *S-N* diagram for the smooth specimens of the non-combustible Mg alloy AMX602B (X=Ca) by the authors (Kitahara et al., 2005; Kitahara et al., 2006; Fujii et al., 2008; Masaki et al., 2008). The relationship between the load stress and the fatigue life of the smooth specimens significantly varies. Moreover, no non-propagating crack was observed in the unbroken specimens. The condition of the surface of the fatigue fracture origin is shown in Fig. 2. The fracture originated at a non-metallic inclusion.

There have been several studies that investigated the effect of the mean stress on the fatigue strength of the conventional Mg alloy (Forrest, 1962; Heywood, 1962; Osgood, 1970; Ogarevic & Stephens, 1990; Akiyama et al., 2000). Forrest (Forrest, 1962) reported that the effect of the mean stress on the fatigue strength of a Mg alloy can be evaluated using the modified Goodman diagram. In contrast, Heywood (Heywood, 1962) and Osgood (Osgood, 1970) reported that the fatigue strength of a Mg alloy under a high mean stress became low and that the fatigue life evaluation using the modified Goodman diagram may not be conservative prediction. However, the reason why the fatigue strength under a high mean stress decreases has not been clarified.

In this study, rotating-bending fatigue tests and tension-compression fatigue tests were carried out on specimens with an artificial defect (a small hole or a small crack). Especially, we examined why the fatigue strength under a high mean stress decreases and whether the fatigue strength at $N = 10^7$ under a mean stress can be applied to an estimation using the modified Goodman diagram. The fatigue testing of the small holed specimens and the small

cracked specimens was first performed, and the characteristics of the fatigue strength at $N = 10^7$ under a high tensile mean stress were investigated. Moreover, the size dependence of the fatigue strength with a small crack was investigated. Based on the results of the fatigue testing of smooth, small hole and the small crack specimens, the influence of the mean stress on the fatigue strength at $N = 10^7$ of the smooth specimens was considered, and the validity of the application of the modified Goodman diagram was investigated.
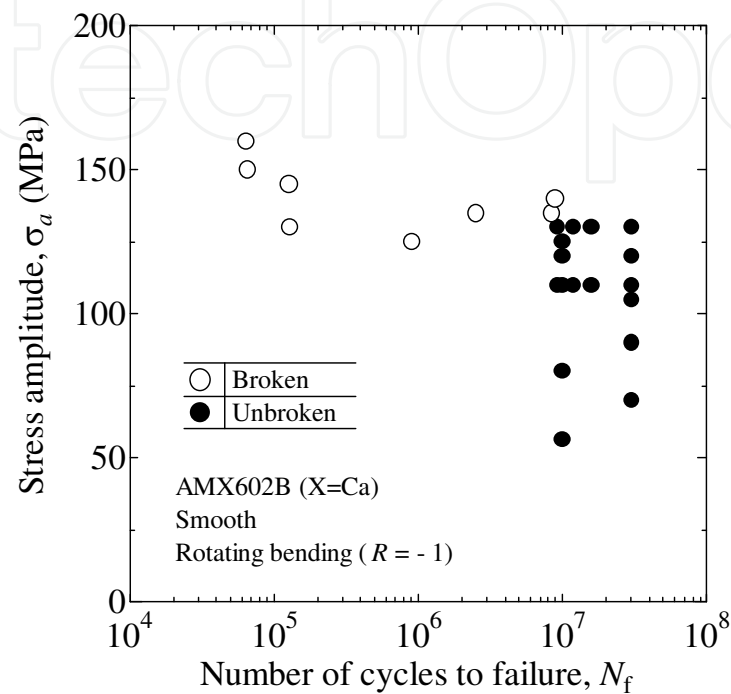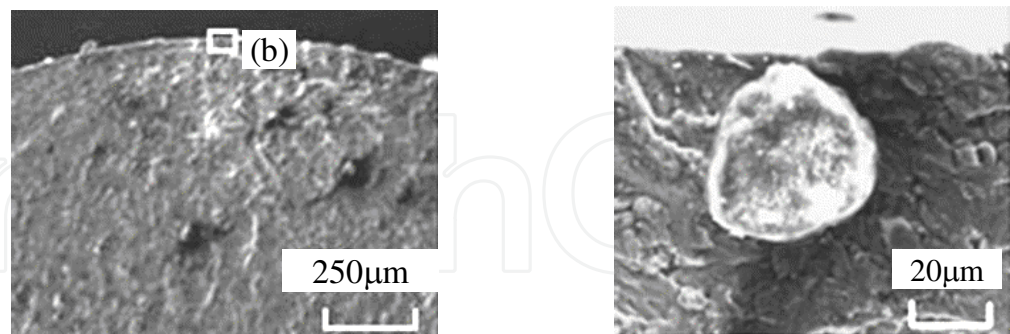

Fig. 1. S-N diagram for the smooth specimens (Kitahara et al., 2005; Kitahara et al., 2006; Masaki et al., 2008)

(a) Fracture surface around the fracture origin   (b) Magnification of fracture origin

Fig. 2. Non-metallic inclusion observed at fatigue fracture origin of the non-combustible Mg alloy (AMX602B (X=Ca)) smooth specimens (rotating-bending) (Kitahara et al., 2005; Kitahara et al., 2006)

2. Characteristics of non-combustible Mg alloy

In order to stop global warming and solve the energy problem, improvement in the fuel consumption by the weight saving of vehicles is now being advanced. In this case, the use of

a magnesium (Mg) alloy is attracting attention because the Clarke number of Mg is high, and Mg has the lowest density of commercial metals.

The non-combustible Mg alloy used in this study is a material which has an improved resistance of being easy to burn by the addition of about 2% calcium (Ca) to the conventional Mg alloy (Sakamoto et al., 1997; Chang et al., 1998; Akiyama et al., 2000; Masaki et al., 2008). Figure 3 shows the relationship between the ignition point and the Ca content of the Mg alloys (Sakamoto et al., 1997). The ignition point of the non-combustible Mg alloy is about 300K higher than that of the conventional Mg alloy. Therefore, the non-combustible Mg alloy can be safely used in casting and metal cutting compared to the conventional Mg alloy. The non-combustible Mg alloy does not need special protection from atmospheric gases or a special flux in the case of casting. Therefore, working in air can be done similar to that for an aluminum alloy. Consequently, an improvement in the problem of high cost, which is one of the concerns of the conventional Mg alloy, is expected.

In order to utilize the non-combustible Mg alloy in practical use as a structural material, it is necessary to determine the fatigue strength characteristics. The fatigue strength characteristics have been investigated for the Mg alloy until now (Forrest, 1962; Heywood, 1962; Osgood, 1970; Ogarevic & Stephens, 1990). The *S-N* diagram characteristics of the Mg alloy are reported as follows: though a clear fatigue limit is not shown, the strength gradually decreases with an increase in the cycles to failure up to a high cycle region (Forrest, 1962; Heywood, 1962; Osgood, 1970; Ogarevic & Stephens, 1990).
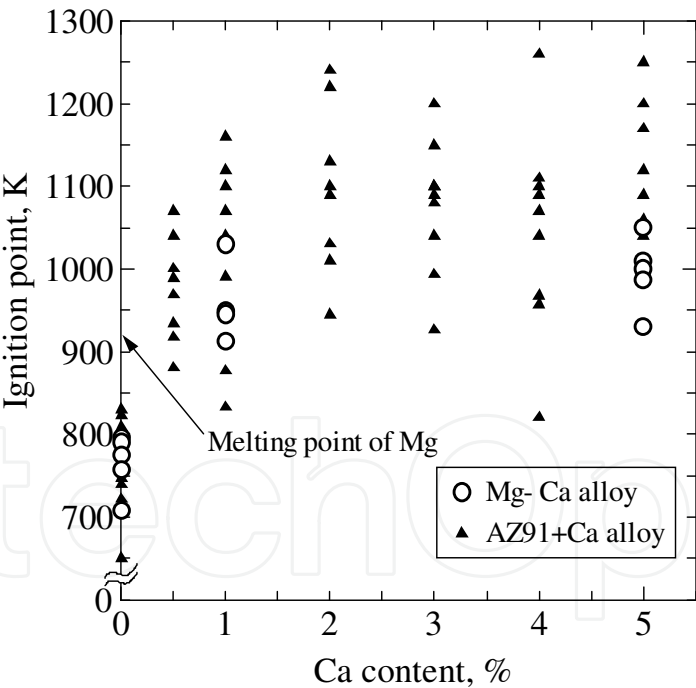

Fig. 3. Relationship between ignition point and Ca content for Mg alloys (Sakamoto et al., 1997)

With the addition of Ca, inclusions increase in the non-combustible Mg alloy (Akiyama et al., 2000). Therefore, it is necessary to consider the influence of inclusions in the case of the fatigue strength characteristics evaluation. The fatigue strength at $N = 10^7$ for the smooth specimens of the three types of the non-combustible Mg alloys (AMX602B (X=Ca), AZX312D (X=Ca), AZX912D (X=Ca)) using a rotating-bending fatigue testing machine was investigated by the authors (Kitahara et al., 2005; Kitahara et al., 2006; Fujii et al., 2008;

Masaki et al., 2008). As a result, it was clarified that the fatigue fracture origin in the non-combustible Mg alloy was due to a non-metallic inclusion as shown in Fig. 2. The non-metallic inclusion is shown in Fig. 2(b). No non-propagating crack at $N = 10^7$ was observed. The fatigue strength at $N = 10^7$ could be estimated using the size of the non-metallic inclusion at the fracture origin (Kitahara et al., 2005; Kitahara et al., 2006). The fatigue strength of the non-combustible Mg alloy was almost the same as that of the conventional Mg alloy.

Figure 4 shows the results of having compared the relationship of the tensile strength and the fatigue strength at $N = 10^7$ in the non-combustible Mg alloy with the relationship of the tensile strength and the fatigue strength at $N = 2×10^7$ for the conventional Mg alloy (Heywood, 1962). Although the fatigue strength at $N = 10^7$ of the non-combustible Mg alloy has some scatter due to the size of the inclusions, it turns out to be comparable to the conventional Mg alloy in tensile strength.
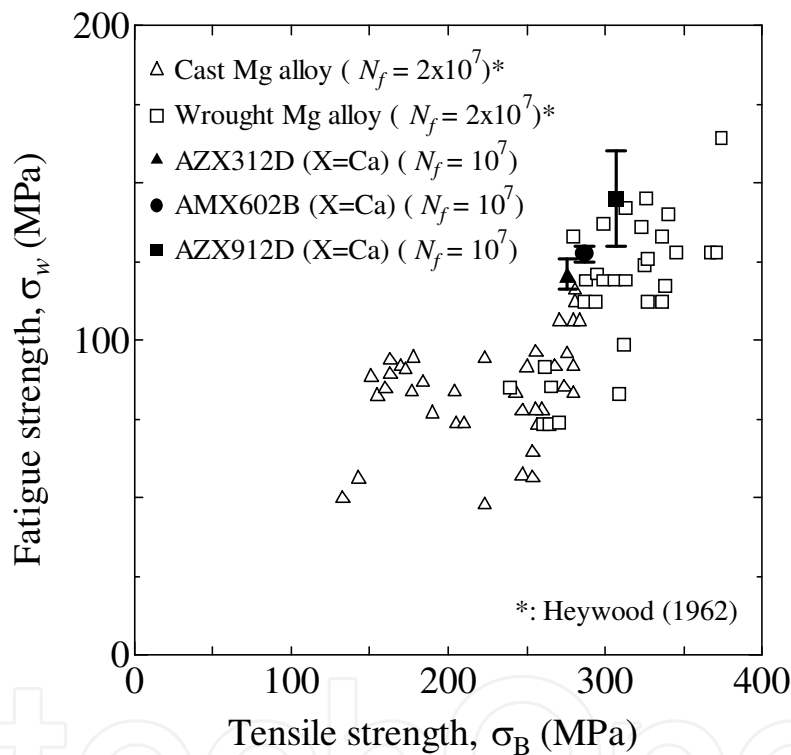

Fig. 4. Relationship between rotating-bending fatigue strength and tensile strength for Mg alloys

3. Experimental procedure

The material used in this study is an extruded non-combustible Mg alloy AMX602B (X=Ca) (extrusion ratio: 3). Its mean grain size is 5 μm. Table 1 shows the chemical composition. Table 2 shows the mechanical properties. Young's modulus, tensile strength and elongation of AMX602B (X=Ca) are the same as those of a conventional Mg alloy. Figure 5 shows the specimen configurations for the rotating-bending fatigue test and tension-compression fatigue test. Three types (smooth, with a small hole and with a small crack) of specimens were prepared. For the non-combustible Mg alloy, if a smooth specimen is used for the

fatigue test, the inclusion of various sizes serves to initiate a fatigue crack, the fatigue strength at $N = 10^7$ varies (Kitahara et al., 2005; Kitahara et al., 2006; Fujii et al., 2008; Masaki et al., 2008), and the influence of the mean stress on the fatigue strength at $N = 10^7$ cannot be studied in detail. In order to correctly determine the fatigue strength at $N = 10^7$, a small hole or a small crack is then introduced in the test specimen. The size of the hole and the crack are slightly larger than the inclusion. This specimen then enabled us to study the influence of the mean stress in detail. Moreover, the reason for having introduced two kinds of artificial defects (a small hole or a small crack) is for the inclusion to clearly show, which is equivalent to a actual defect, a small hole or a small crack.

The surfaces of the specimens are buff-polished using alumina (particle size: 0.05μm). For the small hole specimens, as shown in Fig. 5 (c), a small hole ($d_1 = h_1 = 100$μm) is introduced in the specimen surface after surface polishing. For the small crack specimens, as shown in Fig. 5 (d), a small hole ($d_2 = h_2 = 50$μm) is introduced in the specimen surface after surface polishing, and a small crack ($2a \approx 160$μm) is introduced in the specimen surface by fatigue loading. After that, in order to relieve residual stress caused by introducing the small crack, the specimens are annealed in vacuum for 1 hour at 200°C. The size of the small hole and the small crack are arranged to be the same value: 100μm when the $\sqrt{area}$ parameter model (Murakami, 2002a) is applied. The $\sqrt{area}$ is the square root of the projected "$area$" of an inclusion onto a plane perpendicular to the maximum principal stress. Figure 6 shows the definition of the $\sqrt{area}$. Though we are concerned about the influence on the fatigue strength by the difference in a processing method between each test specimen, it is shown clearly that the influence of vacuum annealing on the fatigue strength at $N = 10^7$ is small (to be described).

Moreover, in order to investigate the size dependence of the fatigue strength of the small crack specimens at $N = 10^7$, the test specimens which have 349μm, 650μm or 918μm length crack were prepared. Rotating-bending fatigue tests were also used for the small crack specimens.

The test machines used for this study are the Ono-type rotating-bending fatigue test machine and the hydro-servo tension-compression fatigue testing machine. Fatigue tests were performed in air at room temperature. The frequency for the rotating-bending fatigue tests is 50Hz, for tension-compression fatigue tests of smooth and the small hole specimens is 20Hz and those for tension-compression fatigue tests of small crack specimens are 30Hz and 35Hz. The replica method was used to observe the specimen surface successively.

Al	Ca	Mn	Zn	Si	Fe	Cu	Ni	Be	Mg
5.98	1.89	0.34	0.002	0.029	<0.001	0.001	<0.001	0.001	Bal.

Table 1. Chemical composition (non-combustible Mg alloy AMX602B (X=Ca))

Young's modulus	Tensile strength	0.2% proof stress	Elongation	Vickers hardness
E (GPa)	σ_B (MPa)	$\sigma_{0.2}$ (MPa)	ε_B (%)	HV (kgf/mm^2)
46	287	210	14	69

Table 2. Mechanical properties (non-combustible Mg alloy AMX602B (X=Ca))

(a) For tension-compression fatigue test (T-C)

(b) For rotating-bending fatigue test (R-B)

(c) Small hole ($d_1 = h_1 = 0.1$)   (d) Small crack ($2a = 0.16, 0.35, 0.65, 0.92$)
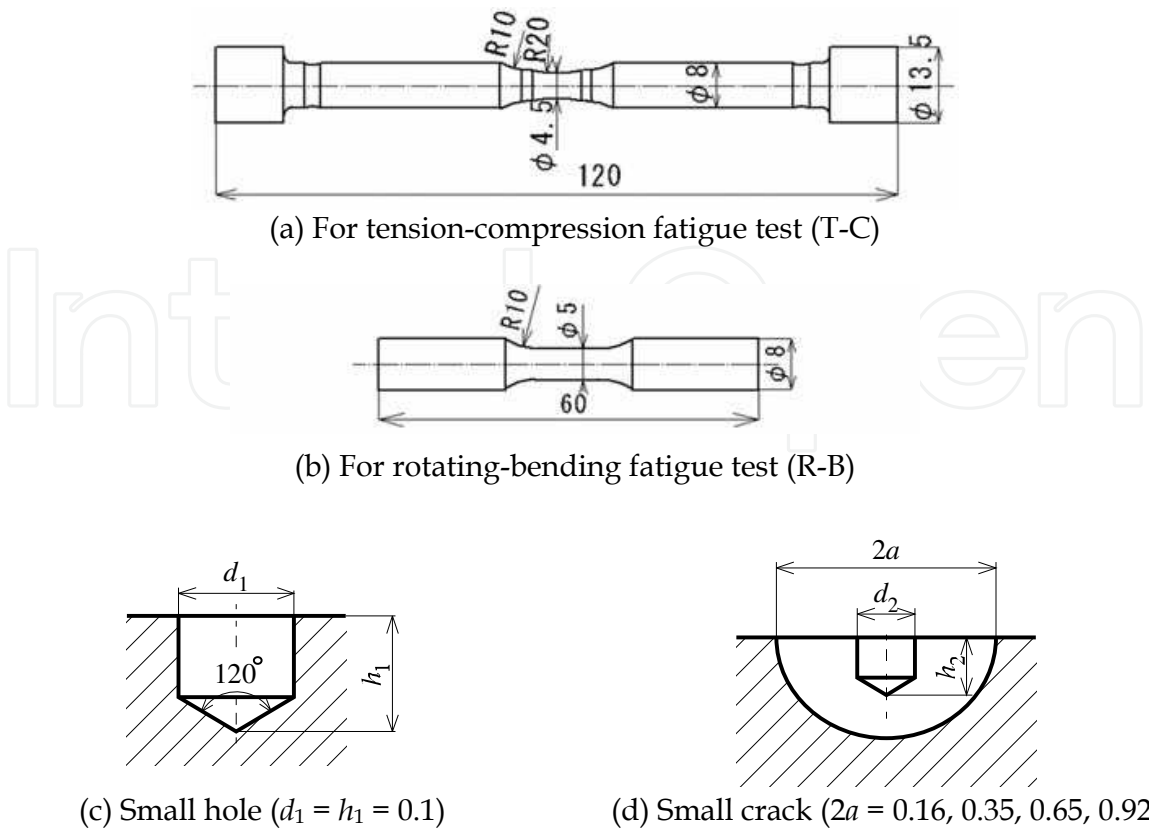
Fig. 5. Shapes and dimensions of the specimens (dimensions in mm)
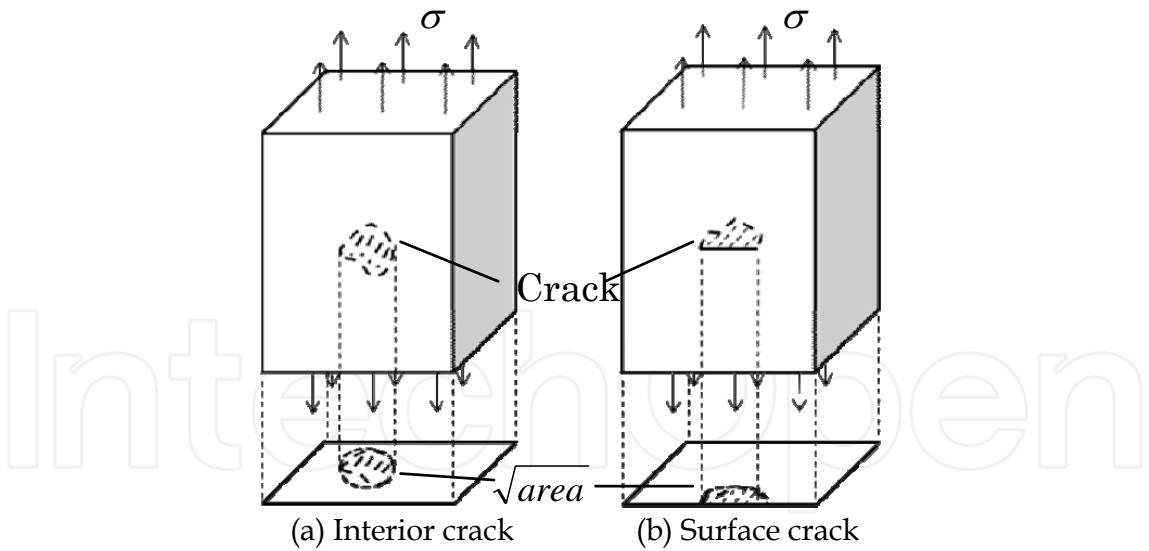

(a) Interior crack   (b) Surface crack

Fig. 6. Definition of $\sqrt{area}$

4. Results and discussion

4.1 Fatigue strength at $N = 10^7$ characteristic of the small hole and the small crack specimens by rotating-bending fatigue test

Figure 7 shows the *S-N* diagram for the specimens with the small hole and the small crack under the rotating-bending fatigue test. In Fig. 7, the results for the vacuum-annealed small

hole specimens are also shown. When vacuum annealing was carried out, we were concerned about the fatigue strength at $N = 10^7$ changing, but in this study, the fatigue strength at $N = 10^7$ after vacuum annealing has not changed. Therefore, the influence on the fatigue strength at $N = 10^7$ by the difference in residual stress of the processing method is small, and we can compare the fatigue strength of the small hole specimens, the small crack specimens and the smooth specimens.
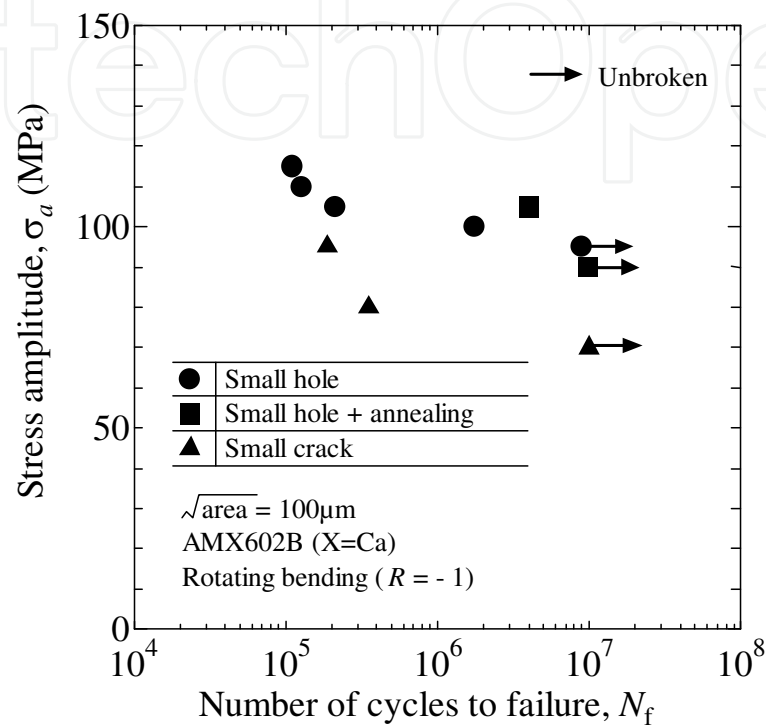

Fig. 7. *S-N* data for the small hole and the small crack specimens

The fatigue strength at $N = 10^7$ of the specimens with the small hole and the small crack was 95MPa and 70MPa, respectively. The fatigue strength at $N = 10^7$ of the specimens with the small hole is about 30% higher than that of the small crack, and effects of defect shape exist (effect of stress concentration level).

Figure 8 shows micrographs around the small hole and the small crack. No crack was observed under the fatigue strength at $N = 10^7$ in the small hole specimen. Otherwise, a nonpropagating crack was observed under the fatigue strength at $N = 10^7$ in the small crack specimen.

Because the small hole specimen and the small crack specimen have a comparable defect size $\sqrt{area}$, when a crack is initiated from the small hole, the stress intensity factor which acts on the crack in the small hole specimen becomes almost equal to the stress intensity factor which acts on the small crack specimen. If one assumes that the crack has been initiated from the small hole, the fatigue strength at $N = 10^7$ of the small hole specimens and the small crack specimen should become comparable. However, in this study, there is about a 30% difference between the fatigue strength at $N = 10^7$ of the small hole specimens and that of the small crack specimens. Therefore, the fatigue strength at $N = 10^7$ of the small hole specimens is determined by the crack-initiating critical stress, and the fatigue strength at $N = 10^7$ of the small crack specimens is determined by the crack-propagating critical stress.

That is, the reason why the fatigue strength at $N = 10^7$ of the small hole specimens is higher than that of the small crack specimens is that the stress amplitude required in order for a crack to be initiated from a small hole is higher than the stress amplitude required for a crack to propagate.

Therefore, effects of the defect shape (effect of stress concentration level) on the fatigue strength at $N = 10^7$ do exist.

4.2 Effect of the mean stress on the fatigue strength at $N = 10^7$ characteristics of the small hole and the small crack specimens

Figure 9 shows endurance data for specimens with a small hole or a small crack. The fatigue strength at $N = 10^7$ of the specimens with a small hole was 30 ~ 150% higher than that of the specimens with a small crack under tensile mean stress. The effects of defect shape (effect of stress concentration level) on the fatigue strength at $N = 10^7$ exist.

On the other hand, when the mean stress is as high as 100MPa or more ($\sigma_m > 100$MPa), the small hole specimens show a different fatigue behavior from that of the small crack specimens. As in the report by Heywood (Heywood, 1962) or Osgood (Osgood, 1970), the fatigue strength at $N = 10^7$ suddenly decreased as the mean stress became high. In order to clarify the reason why only the small hole specimens suddenly decreases in fatigue strength at $N = 10^7$ under a high tensile mean stress, the endurance diagram was considered by dividing it into two domains (Domain I and Domain II).

Domain I is defined as the mean stress $\sigma_m = 0$ to 100MPa domain. This is the domain in which the fatigue strength of the small hole specimens falls gradually and the fatigue strength at $N = 10^7$ of the small crack specimens suddenly decreases compared with the small hole specimens as the mean stress becomes high.

Nisitani & Okasaka (Nisitani & Okasaka, 1973) has reported as follows on the influence of the mean stress affecting the crack initiation and crack propagation. Because the magnitude of stress amplitude is the main factor in crack initiation, the influence of the mean stress is small, and because stress amplitude and the magnitude of the maximum stress are the main factors in crack propagation, the influence of the mean stress is large.

Therefore, because the fatigue strength at $N = 10^7$ of the small hole specimens is the crack-initiation critical stress, the magnitude of stress amplitude becomes important and it is thought that the influence of the mean stress affecting the fatigue strength at $N = 10^7$ of the small hole specimens is small. Moreover, the fatigue strength at $N = 10^7$ of the small crack specimens is the crack-propagation limit; therefore, the stress amplitude and the magnitude of the maximum stress become important, and it is thought that the influence of the mean stress on the fatigue strength at $N = 10^7$ of the small crack specimens is larger than that on the small hole specimens.

Domain II is defined as the mean stress $\sigma_m = 100$ to 190MPa domain. This is the domain in which the fatigue strength of the small hole specimens suddenly decreases and the fatigue strength at $N = 10^7$ of the small crack specimens falls gradually as the mean stress becomes high.

In order to clarify the cause of the fatigue strength at $N = 10^7$ of the small hole specimens suddenly decreasing under a high tensile mean stress, the condition near the small hole in the test was observed in detail. As a result, static cracks from a small hole under a high tensile stress had occurred during the time of the first loading in the fatigue testing. A photograph of the static cracks observed around the small hole is shown in Fig. 10.
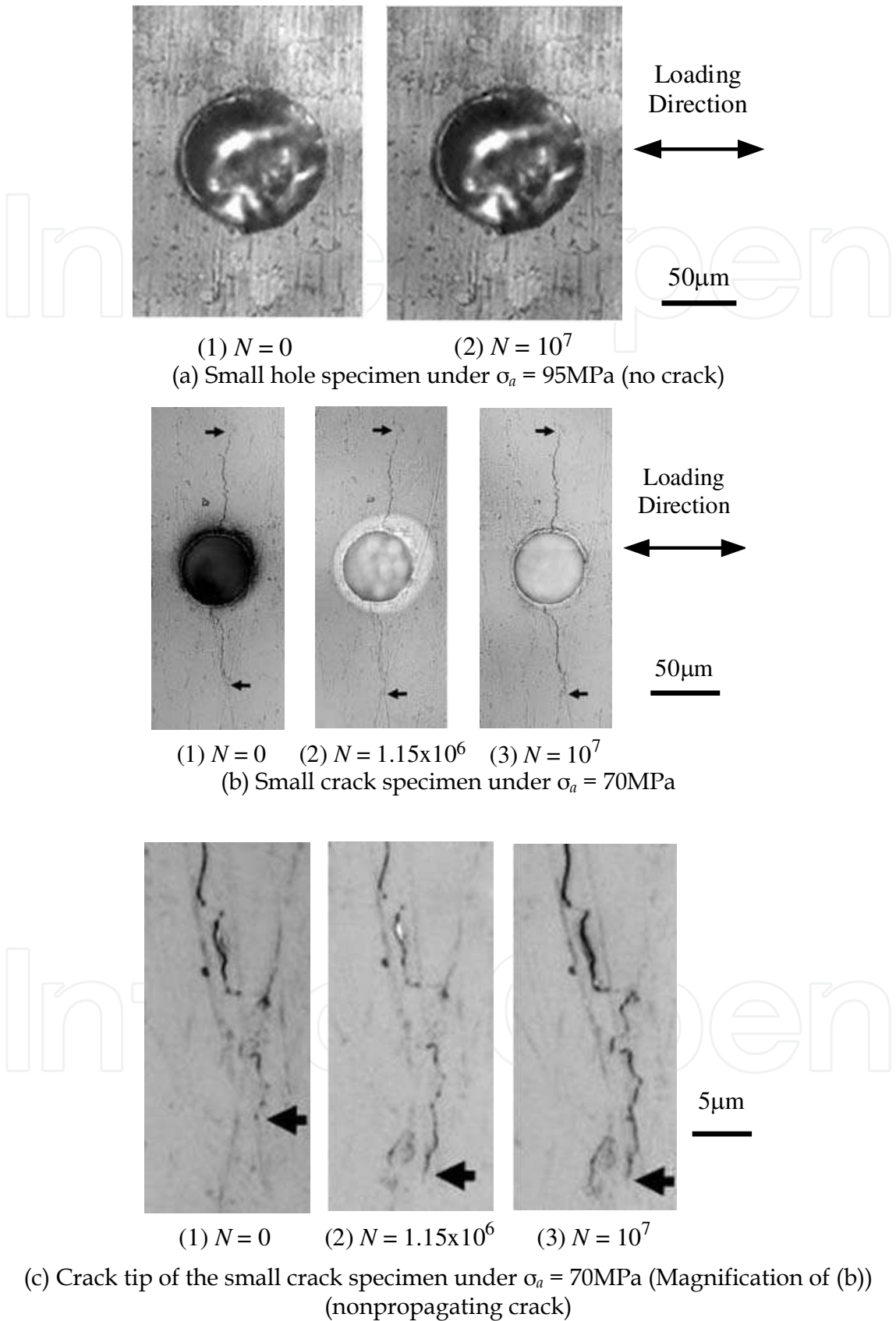
Loading
Direction

50μm

(1) $N = 0$ (2) $N = 10^7$
(a) Small hole specimen under σ_a = 95MPa (no crack)

Loading
Direction

50μm

(1) $N = 0$ (2) $N = 1.15\times10^6$ (3) $N = 10^7$
(b) Small crack specimen under σ_a = 70MPa

5μm

(1) $N = 0$ (2) $N = 1.15\times10^6$ (3) $N = 10^7$

(c) Crack tip of the small crack specimen under σ_a = 70MPa (Magnification of (b))
(nonpropagating crack)

Fig. 8. Micrographs around small hole and small crack (non-combustible Mg alloy AMX602B (X=Ca))
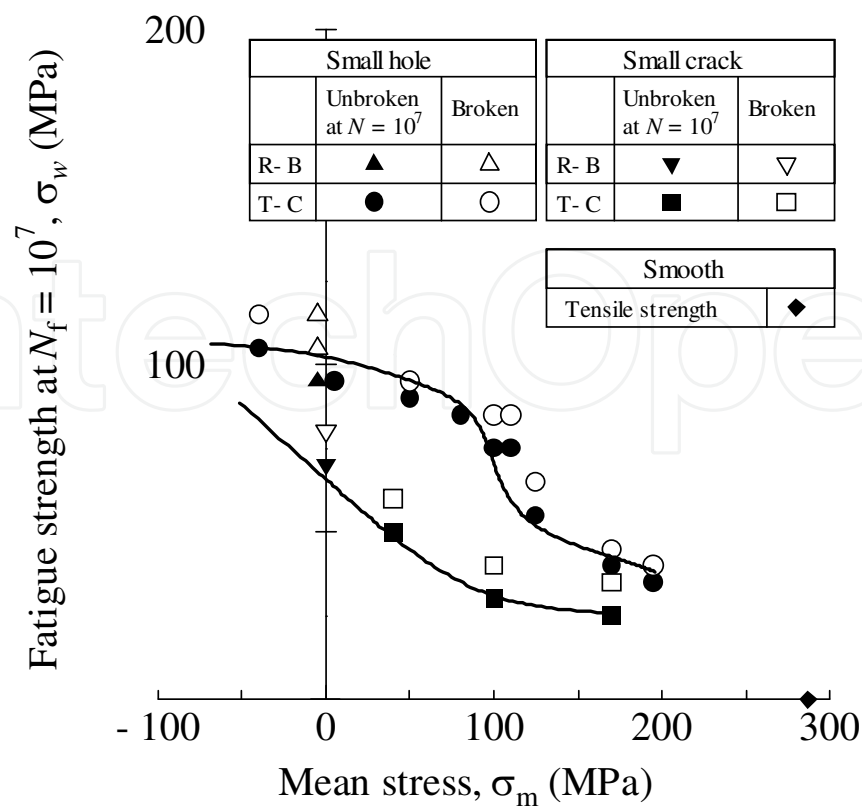
Fig. 9. Endurance data for the small hole and the small crack specimens (non-combustible Mg alloy AMX602B (X=Ca))

As shown in Fig. 9, the fatigue strength at $N = 10^7$ of the small hole specimens is higher than the fatigue strength at $N = 10^7$ of the small crack specimens by about 30 ~ 150%, and it shows the influence of defect shape (effect of stress concentration level). Therefore, the reason that the fatigue strength at $N = 10^7$ suddenly decreases under a high tensile mean stress in the small hole specimens is as follows: it falls when the shape of the defect changes from a small hole to a small crack and the fatigue strength at $N = 10^7$ of the small hole specimens approaches the fatigue strength at $N = 10^7$ of the small crack specimens, because static cracks were initiated from a small hole during the time of the first loading. That is, in the small hole specimens, unless it comes under a high tensile mean stress during which static cracks are initiated from the small hole, the fatigue strength at $N = 10^7$ does not fall. Kang et al. (Kang et al., 2007) has also reported that the fatigue limit fell due to a static crack in research on high strength prestrained steel.

In addition, the reason why the fatigue strength at $N = 10^7$ of the small hole specimens is slightly higher under a high tensile mean stress than the fatigue strength at $N = 10^7$ of the small crack specimens is considered to be as follows. The crack initiated in the small hole specimens at the time of the first loading is not a fatigue crack but a static crack, and the static crack has been strongly influenced by crack closure due to plastic deformation near the small hole, so that the crack opening stress is then higher than that of the small crack specimens.

Kondo et al. (Kondo et al., 2003) has reported the small crack opening stress of steel as follows regarding the fatigue strength characteristics of the small crack specimens under a high tensile mean stress ($R = 0.5$): under a high mean stress, the crack closure is not

(a) $\sigma = 0$ MPa ($N = 0$)

Loading
Direction

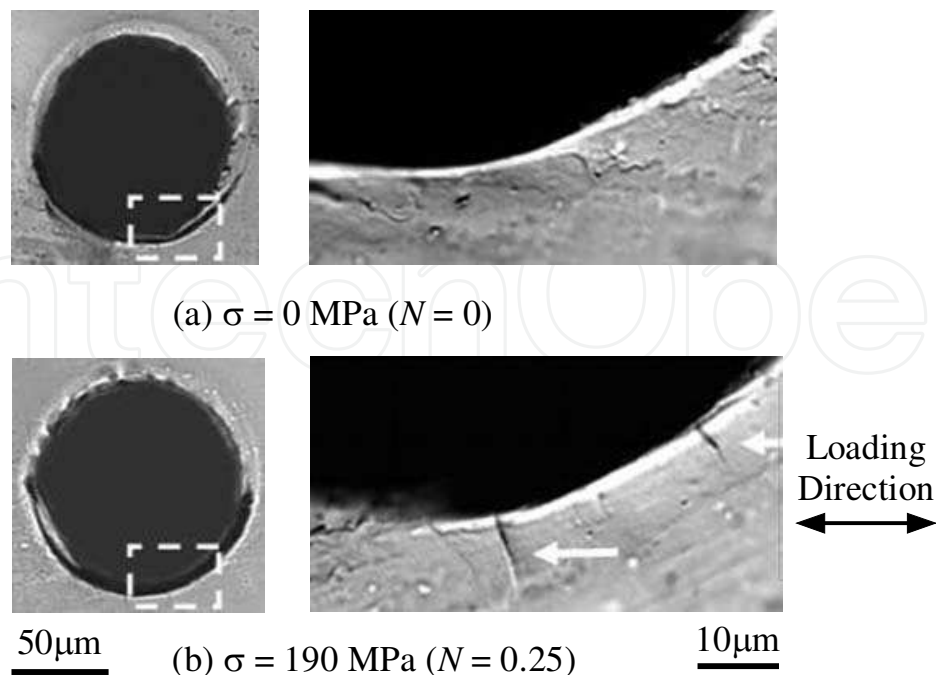50μm   (b) $\sigma = 190$ MPa ($N = 0.25$)   10μm

Fig. 10. Micrographs of static cracks observed during the first loading (arrow indicates static crack)

observed, so that the threshold stress intensity factor range, ΔK_{th} is the same value as the effective threshold stress intensity factor range, $\Delta K_{eff, th}$.

Therefore, the reason why the fatigue strength at $N = 10^7$ of the small crack specimens falls gradually in this research is considered to be because the fatigue strength at $N = 10^7$ of the small crack specimens becomes close to the effective threshold stress intensity factor range, $\Delta K_{eff, th}$, for a high tensile mean stress.

Figure 11 shows the relationship between the defect size $\sqrt{area}$ of the smooth specimens, the small hole specimens and the small crack specimens and their fatigue strength. In order to compare the fatigue strength of the smooth specimens with the results for the small crack specimens, the results of extrapolating the relation between the defect size $\sqrt{area}$ and the fatigue strength at $N = 10^7$ using the experimental results for a crack length of about 50μm ($\sqrt{area}$ = 30μm) in which crack length is sufficiently larger than the size of a few grain are shown. The slope of extrapolation was set to 1/6 (Murakami, 2002b) which reported to be good agreement with many materials.

The relationship for the smooth specimens between the defect size $\sqrt{area}$ and the fatigue strength is closer to the relationship for the small hole specimens than the relationship for the small crack specimens. Moreover, the fatigue strength at $N = 10^7$ of the smooth specimens is high compared with that of the small crack specimens. Therefore, it is thought that in the fatigue strength at $N = 10^7$, the fatigue behavior of the smooth specimens shows the near fatigue behavior of the small hole specimens. That is, the fatigue strength at $N = 10^7$ of the smooth specimens is thought to be the crack initiation limit. The effect of the mean stress on the fatigue strength at $N = 10^7$ is considered as follows. Under the high mean stress in which a static crack is initiated, the fatigue strength at $N = 10^7$ falls; however, the fall in fatigue strength at $N = 10^7$ is smooth under the mean stress in which a static crack is not
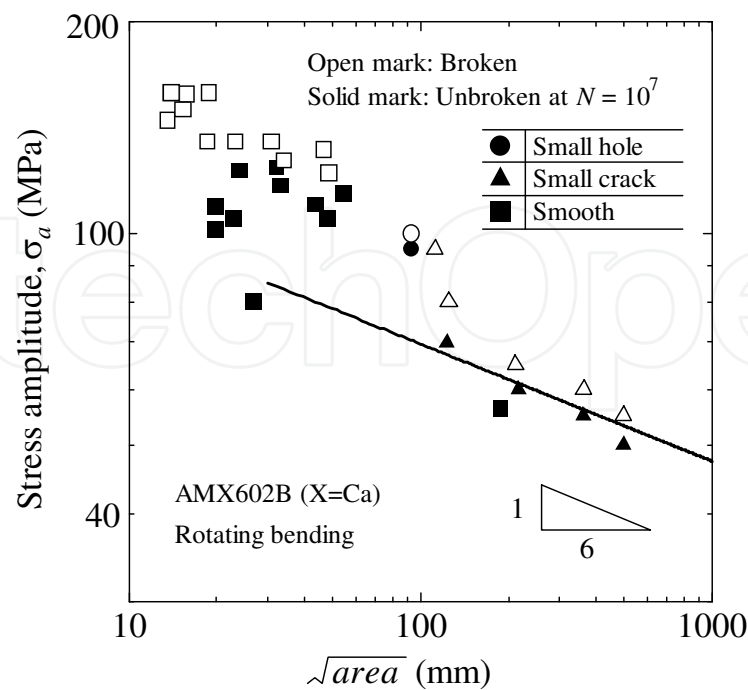
Fig. 11. Relationship between stress amplitude and defect size

initiated. Like the fatigue behavior of the small hole specimens, unless it is examined on the smooth specimens, a nonpropagating crack is indeed not observed. As shown in Fig. 12, when the loading of the high tensile stress was carried out, the static crack was initiated from the inclusion.

4.3 Application validity of the modified Goodman diagram

Figure 13 shows the endurance data for the smooth specimens. In the fatigue test results for the smooth specimens, the highest fatigue strength at $N = 10^7$ was applied, because the application of the highest fatigue strength created a severe modified Goodman diagram. The fatigue strength at $N = 10^7$ of the small hole specimens (Fig. 5) is also shown in the figure by a dashed line. The fatigue strength at $N = 10^7$ of the smooth specimens is higher than that of the small hole specimens in the range of $\sigma_{max} < \sigma_{0.2}$. From these results, the mean stress influence on the fatigue strength at $N = 10^7$ can be evaluated on the safety side using the modified Goodman diagram in the practical stress range ($\sigma_{max} < \sigma_{0.2}$).

Meanwhile, a static crack is initiated also in the smooth specimens, and there is a possibility that the fatigue strength at $N = 10^7$ may suddenly decrease under a high tensile mean stress. However, the tensile stress at which a static crack is initiated in a smooth specimens exceeds 0.2% proof stress, and the range under the mean stress which is considered to cause the fall fatigue strength at $N = 10^7$ in the smooth specimens is not a practical stress range ($\sigma_{max} < \sigma_{0.2}$).

4.4 Discussion of the effect of the mean stress on the fatigue strength of other Mg alloys

The possibility that the fatigue strength falls due to a static crack initiated under a high tensile mean stress in other Mg alloys is considered. In order for the fatigue strength to fall due to a static crack, the following two points are required. (i) The static crack is initiated by

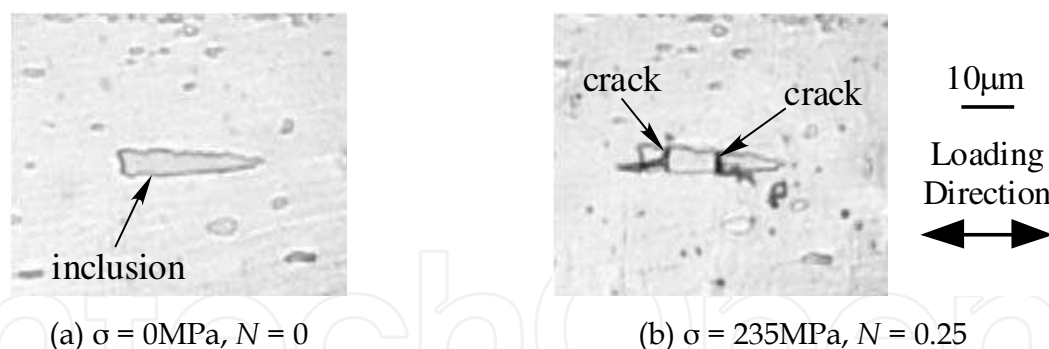(a) σ = 0MPa, N = 0   (b) σ = 235MPa, N = 0.25

Fig. 12. Small static cracks initiated from inclusion at the first loading (non-combustible Mg alloy AMX602B (X=Ca))

the loading of a high tensile stress. (ii) The crack-initiation critical stress is higher than the fatigue crack-propagation critical stress, and once a crack is initiated, the fatigue strength will fall.

Elongation of many Mg alloys is about 10% (The Japan Magnesium Association, 2000). Because the elongation is small, it is thought that a static crack is initiated by a high tensile stress load. Moreover, because a clear fatigue limit is not defined for smooth specimens of many Mg alloys, the crack-initiation critical stress of the smooth specimens is higher than the fatigue crack-propagation critical stress, and once a crack is initiated, the fatigue strength is thought to fall.

Therefore, also in other Mg alloys, it is thought that the fatigue strength falls due to static crack initiation like that in the small hole specimens in this research. One can say that, also in other Mg alloys, unless the alloy is under a high tensile mean stress during which a static crack is initiated, it is thought that the influence of the mean stress on the fatigue strength can be evaluated using the modified Goodman diagram.

Furthermore, the difference in the opinions of Forrest (Forrest, 1962), Heywood (Heywood, 1962) and Osgood (Osgood, 1970) can also be explained based on the considerations described above. The report of Forrest (Forrest, 1962) summarized the influence of the mean stress on the fatigue strength of the Mg alloy which does not have much of a difference in the fatigue crack-propagation critical stress and the crack-initiation critical stress, and it is thought that the fatigue strength did not suddenly decrease under the high tensile mean stress. The reports of Heywood (Heywood, 1962) and Osgood (Osgood, 1970) summarized the influence of the mean stress affecting the fatigue strength of the Mg alloy which shows a difference in the fatigue crack-propagation critical stress and the crack-initiation critical stress, and the fatigue strength suddenly decrease under the high tensile mean stress; if the modified Goodman diagram is used for evaluation of fatigue strength, it is thought that it may not be conservative prediction.

5. Conclusions

Using the smooth specimens, the small hole specimens and the small crack specimens of the non-combustible Mg alloy AMX602B (X=Ca), the influence of the mean stress on the fatigue strength at $N = 10^7$ was investigated. We especially investigated the validity of applying the modified Goodman diagram to determine why the fatigue strength suddenly decreases

under a high tensile mean stress and why the mean stress affected the fatigue strength at $N = 10^7$. The conclusions are as follows.

1. We proposed an evaluation method for the mean stress effect of the inclusion-induced scattered fatigue strength. The proposed method involves fatigue testing using specimens with an artificial defect.

2. Using the non-combustible Mg alloy, whose fatigue strength shows an inclusion-induced scattering, the mean stress effect of the fatigue strength was evaluated.

3. In the range of $\sigma_m = 0$ to 100MPa, the fatigue strength at $N = 10^7$ of the small hole specimens was higher than that of the small crack specimens by 30 to 150%.

4. In the range of $\sigma_m > 100$MPa, the fatigue strength at $N = 10^7$ of the small hole specimens suddenly decreased due to static cracks initiating around the small hole during the first loading.

5. In the practical stress range ($\sigma_{max} < \sigma_{0.2}$), the fatigue strength at $N = 10^7$ of the smooth specimens was estimated using the modified Goodman diagram.
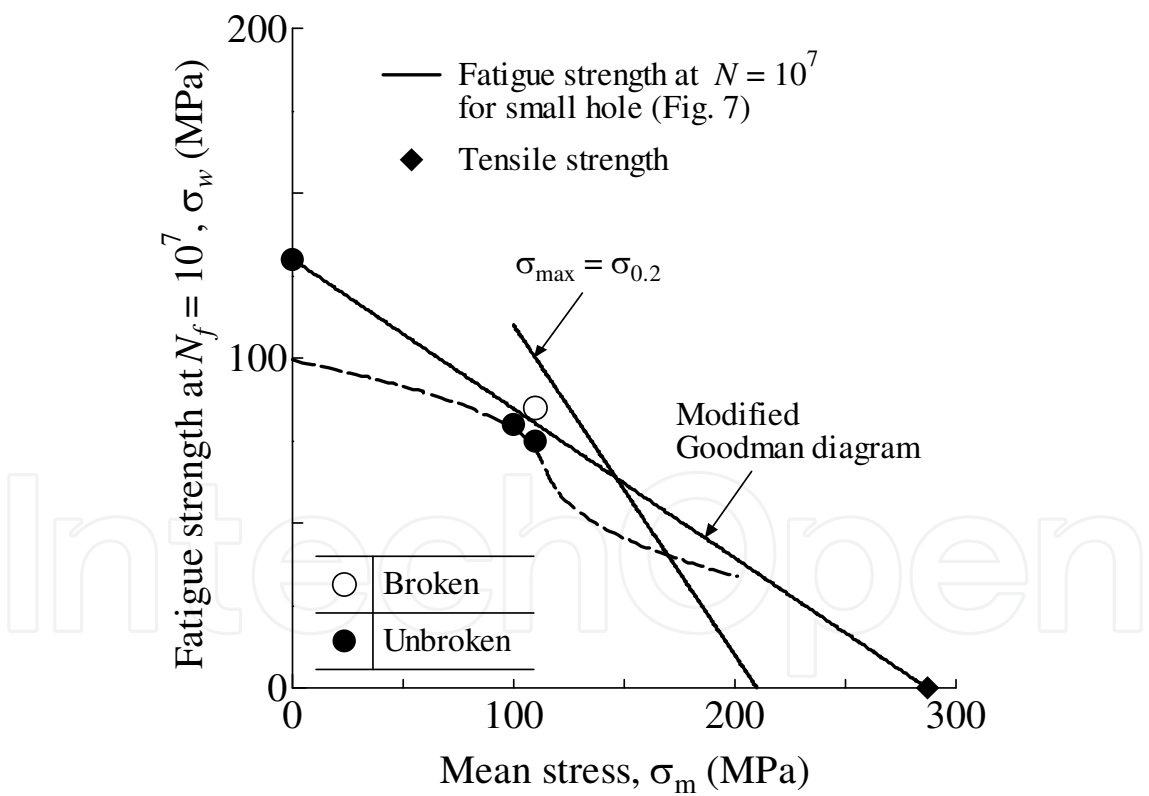
Fig. 13. Endurance data for the smooth specimens (non-combustible Mg alloy AMX602B (X=Ca))

6. References

Akiyama, S., Ueno, H. & Sakamoto, M. (2000). Purification of Molten Non-combustible Magnesium Alloy (in Japanesea). *Journal of Japan Foundry Engineering Society*, Vol. 72, No. 8 (521-524), ISSN: 13420429

Chang, S-Y., Matsushita, M., Tezuka, H. & Kamio, A. (1998). Ignition prevention of magnesium by simultaneous adding of calcium and zirconium. *International Journal of Cast Metals Research*, Vol. 10, No. 6 (345-351), ISSN: 13640461

Forrest, P. G. (1962). *Fatigue of Metals*, Pergamon Press, ISBN: 0080097294, Oxford, (75, 95-103)

Fujii, T., Morishige, K., Hamada, S., Noguchi, H., Sakamoto, M. and Ueno, H. (2008). Fatigue Strength Characteristics of Non-Combustible Mg Alloy. *Journal of Solid Mechanics and Materials Engineering*, Vol. 2, No. 6 (763-770) ISSN: 18809871

Heywood, R. B. (1962). Designing Against Fatigue, Chapman and Hall Ltd., ISBN: 0412068206, London, (69-70)

Kang, M., Aono, Y. & Noguchi, H. (2007). Effect of prestrain on and prediction of fatigue limit in carbon steel. *International Journal of Fatigue*, Vol. 29, No. 9-11 (1855-1862) ISSN: 01421123

Kitahara, Y., Shimazaki, H., Yabu, T., Noguchi, H., Sakamoto, M. &Ueno H. (2005). Influence of inclusions on fatigue characteristics of non-combutible Mg alloy. *Materials Science Forum*, Vol. 482 (359-362) ISSN: 02555476

Kitahara, Y., Ikeda, K., Shimazaki, H., Noguchi, H., Sakamoto, M. & Ueno H. (2006). Fatigue strength characteristics of non-combustible Mg alloy: 1st report, quantitative comparison among fatigue strengths of three non-combustible Mg alloys (in Japanese). *Transactions of the Japan Society of Mechanical Engineers A*, Vol. 72, No. 717 (661-668) ISSN: 03875008

Kondo, Y., Sakae, C., Kubota, M. & Kudou T. (2003). The effect of material hardness and mean stress on the fatigue limit of steels containing small defects. *Fatigue and Fracture of Engineering Materials and Structures*, Vol. 26, No. 8 (675-682) ISSN: 8756758X

Masaki, K., Ochi, Y., Kakiuchi, T., Kurata K., Hirasawa, T., Matsumura, T., Takigawa, Y. & Higashi, K. (2008). High Cycle Fatigue Property of Extruded Non-Combustible Mg Alloy AMCa602. *Materials Transactions*, Vol. 49, No. 5 (1148-1156) ISSN: 13459678

Murakami, Y. (2002a). *Metal Fatigue: Effects of Small Defects and Nonmetallic inclusions*, Elsevier, ISBN: 0080440649, Amsterdam, (16-19)

Murakami, Y. (2002b). *Metal Fatigue: Effects of Small Defects and Nonmetallic inclusions*, Elsevier, ISBN: 0080440649, Amsterdam, (60-62)

Nisitani, H. & Okasaka, K. (1973). Effect of mean stress on fatigue strength crack strength and notch radius at branch point, under repeated axial stresses. *Transactions of the Japan Society of Mechanical Engineers*, Vol. 39, No. 317 (49-59) ISSN: 00290270

Ogarevic, V. V. & Stephens, R. I. (1990). Fatigue of magnesium alloys. *Annual Review of Materials Science*, Vol. 20, No. 1 (141-177), ISSN: 00846600

Osgood C. C. (1970). Fatigue Design, Wiley-Interscience, ISBN: 0471657115, New York, (433-439)

Sakamoto, M., Akiyama, S., Hagio, T. & Ogi, K. (1997). Control of oxidation surface film and suppression of ignition of molten Mg-Ca alloy by Ca addition (in Japanesea). *Journal of Japan Foundry Engineering Society*, Vol. 69, No. 3 (227-233) ISSN: 13420429

The Japan Magnesium Association (2000). *Handbook of advanced magnesium technology (in Japanese)*, Kallos Publishing, ISBN: 4874320147, Tokyo, (447-460)
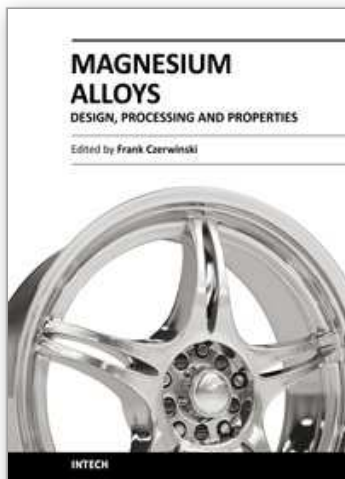
Magnesium Alloys - Design, Processing and Properties

Edited by Frank Czerwinski

Scientists and engineers for decades searched to utilize magnesium, known of its low density, for light-weighting in many industrial sectors. This book provides a broad review of recent global developments in theory and practice of modern magnesium alloys. It covers fundamental aspects of alloy strengthening, recrystallization, details of microstructure and a unique role of grain refinement. The theory is linked with elements of alloy design and specific properties, including fatigue and creep resistance. Also technologies of alloy formation and processing, such as sheet rolling, semi-solid forming, welding and joining are considered. An opportunity of creation the metal matrix composite based on magnesium matrix is described along with carbon nanotubes as an effective reinforcement. A mixture of science and technology makes this book very useful for professionals from academia and industry.

How to reference

In order to correctly reference this scholarly work, feel free to copy and paste the following:

INTECH
open science | open minds